Modern Digital Seismology — Instrumentation, and Small Amplitude Studies in the Engineering World

Thesis by

John F. Clinton

In Partial Fulfillment of the Requirements

for the Degree of

Doctor of Philosophy

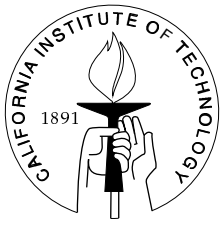

California Institute of Technology

Pasadena, California

2004

(Submitted May 24, 2004)

© 2004

John F. Clinton

All Rights Reserved

Acknowledgements

I would like to thank my advisor, Tom Heaton. Throughout my time at Caltech, he was continuously jovial, and gave me great encouragement. He has always been overly generous with his time, and I have learnt much from our frequent discussions.

I would like to acknowledge Jascha Polet and David Johnson from SeismoLab, who taught me a lot about the hardware and software issues, helped set up countless experiments, and were always helpful with data analysis and recovery. I also would like to thank Arnie Acosta and Erdal Safak for their help with obtaining data from the USGS array at Millikan Library. Mr. Isamu Yokoi from Tokyo-Sokushin was also extremenly helpful with all issues that arose with the VSE sensors. I would like to thank IRIS for purchasing the VSE-355G2 sensor.

The faculty and students of Civil Engineering also provided great support. In particular Brad Aagaard for the brains, Andy for the sharing the misery at 2am all first and second years long, Swami, Javier and Case for the laughs. And especially Case for the extensive proof-reading.

My mother-in-law, Maria Cua, helped out with minding Peete, letting us get some work done.

My parents, Peter and Margaret, so far away for these past years, have yet managed to share much of my Caltech experience, and helped me make it to the end.

But after everyone has gone home, Peete and Georgie were always there, and allowed me to too often not go home myself. Thanks for your patience and love. For what its worth, this is for both of you.

Abstract

The recording of ground motions is a fundamental part of both seismology and earthquake engineering. The current state-of-the-art 24-bit continuously recording seismic station is described, with particular attention to the frequency range and dynamic range of the seismic sensors typically installed. An alternative method of recording the strong-motions would be to deploy a velocity sensor rather than an accelerometer. This instrument has the required ability to measure the strongest earth motions, with enhanced long period sensitivity.

An existing strong motion velocity sensor from Japan was tested for potential use in US seismic networks. It was found to be incapable of recording strong motions typically observed in the near field of even moderate earthquakes. The instrument was widely deployed near the M8.3 Sept 2003 Tokachi-Oki earthquake. The dataset corroborated our laboratory observations of low velocity saturations. The dataset also served to show all inertial sensors are equally sensitive to tilting, which is widespread in large earthquakes. High-rate GPS data is also recorded during the event. Co-locating high-rate GPS with strong motion sensors is suggested to be currently the optimal method by which the complete and unambiguous deformation field at a station can be recorded.

A new application of the modern seismic station is to locate them inside structures. A test station on the 9^{th} floor of Millikan Library is analysed. The continuous data-stream facilitates analysis of the building response to ambient weather, forced vibration tests, and small earthquakes that have occurred during its lifetime. The structure's natural frequencies are shown to be sensitive not only to earthquake excitation, but rainfall, temperature and wind. This has important implications on structural health monitoring, which assumes the natural frequencies of a structure do not vary significantly unless there is structural damage.

Moderate to small earthquakes are now regularly recorded by dense, high dynamic range networks. This enhanced recording of the earthquake and its aftershock sequences makes possible the development of a Green's Function deconvolution approach for determining rupture parameters.

Contents

Acknowledgements **iii**

Abstract **iv**

1 Introduction **1**

1.1 Seismological Instrumentation 1

1.2 Applications of Modern Instrument Data 3

1.2.1 Small Amplitude Studies for Buildings 3

1.2.2 Moderate Earthquake Source Inversions 3

1.3 A Comment on Deconvolutions 4

1.4 A Comment on Tilt 7

1.5 A Simple Methodology for Determining Displacement and Tilt Using Seismometers and GPS 10

1.6 A Summary of Recommendations for Modern Station Design 12

1.6.1 Station options 13

2 A Strong Motion Velocity Meter in a Modern Seismic Network? **17**

2.1 Introduction 17

2.2 A Typical CISN Station 20

2.3 The Definition of Dynamic Range 27

2.4 The Seismographic System 28

2.4.1 Dynamic Range of the Digital Recorder 29

2.4.2 Dynamic Range of Each Seismometer 30

2.5 Strong Motion Instrument Comparisons Using Recorded Earthquake Signals 34

2.5.1 Assembly of the Earthquake Database 34

2.5.2 Recovery of Earth Signals 36

2.5.3 Recovery of Acceleration 41
2.6 'Strong Motion' Recordings at Teleseismic Distances 42
2.7 Summary 44

3 Examination of a Strong Motion Velocity Instrument 46
3.1 Introduction 46
3.2 A Note on Removing the Instrument Response 48
3.2.1 Time Domain Deconvolution: Direct Integration 52
3.2.2 Frequency Domain Deconvolution, Division by the Instrument Response 56
3.3 Synthetic Responses for the VSE-355G2 and FBA-23 59
3.4 Instrument Design and Specifications 66
3.5 Test Data and Analysis 69
3.5.1 Instrument Sensitivity 69
3.5.2 Instrument Response 71
3.5.3 Instrument Resolution 74
3.5.4 Instrument Clipping 78
3.5.5 Spurious Resonances 84
3.6 Recovery of Teleseismic Data 85
3.7 Summary 86

4 Strong Motion Velocity Instrument Performance in 2003 M8.3 Tokachi-Oki Earthquake 90
4.1 Introduction 90
4.2 The Available Networks 92
4.2.1 F-Net 92
4.2.2 K-Net 92
4.2.3 KiK-Net 92
4.2.4 WISE 95
4.3 Static Offset — GPS and Seismometers 96
4.4 Strong Motion around Hokkaido 108

4.4.1 Stations near Kushiro town . . . 109
4.4.2 Stations near Samani town . . . 113
4.4.3 Stations near Erimo . . . 127
4.4.4 Stations near Urahoro . . . 132
4.4.5 Stations near Obihiro . . . 144
4.5 Other F-Net stations on Hokkaido . . . 149
4.6 Teleseismic Motion around Japan . . . 152
4.7 Summary . . . 172

5 Modifications to the VSE-355G2 — The VSE-355G3 176
5.1 Introduction . . . 176
5.2 Modifications . . . 177
5.3 Test Analysis . . . 178
5.3.1 Instrument Clipping . . . 178
5.3.2 Instrument Response . . . 183
5.3.3 Instrument Sensitivity . . . 186
5.4 Summary . . . 195

6 Small Amplitude Studies in Structures 199
6.1 Introduction . . . 199
6.2 Historical Evidence for Natural Frequency Wandering — Millikan Library . 201
6.3 The Current System of Instrumentation at Caltech . . . 211
6.3.1 Millikan Library (MIK, USGS-Caltech Array) . . . 212
6.3.2 Broad Center (CBC) . . . 212
6.3.3 525 S. Wilson Ave — USGS Office (GSA) . . . 215
6.3.4 Robinson Building (CRP) . . . 215
6.3.5 The Athenaeum (CAC) . . . 217
6.4 Analysis of the Continuous Data Streams . . . 217
6.4.1 Entire Station Duration — MIK and CBC . . . 218
6.4.2 Winter Storms — MIK . . . 225
6.4.3 Santa Ana Winds — MIK . . . 232

6.4.4 Diurnal Variation and High Temperatures — MIK 232
6.5 M5.4 22 February 2003 Big Bear Sequence 235
6.5.1 Millikan Library 235
6.5.2 Broad Center 239
6.6 A Linear Transfer Function Solution? 239
6.7 Conclusions and Discussion 243

7 Source Time Functions **249**
7.1 Introduction 249
7.2 Theory and Methodology 250
7.2.1 Directivity 255
7.3 Sample Events 260
7.3.1 Yorba Linda 260
7.3.2 Big Bear 275
7.3.3 Anza 280
7.4 Conclusions and Discussion 285

Bibliography **290**

A VSE-355G2/3 Testing Regime **296**
A.1 12 December 2001: DSN — Noise and Track Test 296
A.2 February - March 2002: PASA — Noise and Screw Test 299
A.3 March 2002: PASB — Noise and Calibration Coil Test 299
A.4 8 March 2002: DSN — Cart Test I 301
A.5 June 2002: DSN — Cart Test II 301
A.6 June - September 2002: Japan 302
A.7 11 - 12 November 2002: DSN — Cart Test III 302
A.8 27 November 2002: DSN — Cart Test IV 302
A.9 12 March 2003: DSN — Cart Test V 302
A.10 26 March 2003: DSN — Cart Test VI 303
A.11 April - June 2003: Japan 303

A.12 15 - 16 September 2003: DSN — Cart Test VI 303
A.13 October - November 2003: CRP 308
A.14 24 - 26 November 2003: CRP and DSN 308
A.15 23 January 2004: CRP and DSN 314

B Previous Studies of Millikan Library **317**

C Millikan Library Dynamic Response to Forced Vibration **323**

List of Figures

1.1 The effect of tilt on seismometers 9

2.1 Typical CISN station recording range 22
2.2 SCSN station map - entire region 24
2.3 SCSN station map - Los Angeles basin 25
2.4 Broadband instrument response 26
2.5 Accelerometer noise floors 31
2.6 Instrument responses 33
2.7 Sample bandpasses for M3.5 at 100km 37
2.8 Sample bandpasses for M7.5 at 10km 38
2.9 Data scatter and geometric mean for M3.5 at 100km 39
2.10 Frequency - amplitude plot — advantages of recording velocity 40
2.11 Comparison of acceleration records for an accelerometer and a broadband velocity meter 42
2.12 Velocity time series from a large teleseism 43
2.13 As Figure 2.12, bandpass from 37.5s to 75s 43
2.14 As Figure 2.12, bandpass from 75s to 150s 44

3.1 VSE-355G2 photo - Cart Test setup 46
3.2 Time domain deconvolution of a strong motion record 55
3.3 Time and frequency domain deconvolution comparison: strong motion record 57
3.4 Time and frequency domain deconvolution comparison: regional motions . 58
3.5 Synthetic instrument response to a δ-function in acceleration 61
3.6 Synthetic instrument response to a step-function in acceleration 62
3.7 Synthetic instrument response to a static offset in acceleration, with a ramp 63
3.8 Synthetic instrument response to step function in displacement 64
3.9 Synthetic instrument response to static offset in displacement, with ramp . . 65

3.10 Synthetic instrument response idealised cart test 67
3.11 Sensitivity scaling (VSE-355G2) 70
3.12 Calibration coil response (VSE-355G2) 73
3.13 Comparison of theoretical and observed response (VSE-355G2) 74
3.14 Instrument resolution — E-W component (VSE-355G2) 75
3.15 Instrument resolution — N-S component (VSE-355G2) 75
3.16 Instrument resolution — Z component (VSE-355G2) 76
3.17 Instrument resolution at high frequency (VSE-355G2) 77
3.18 Frequency - amplitude (VSE-355G2) 79
3.19 Comparison of VSE / FBA noise floors, as Fig. 3.18 (VSE-355G2) 80
3.20 Accelerometer noise floors, as Fig. 3.18 (VSE-355G2) 80
3.21 Cart Test — uncorrected instrument clip (VSE-355G2), April 2002 82
3.22 Calibration test — clipping (VSE-355G2) 83
3.23 Cart Test — 'corrected' instrument — no $15cm/s$ clip (VSE-355G2) 84
3.24 Cart Test — 'corrected' instrument — clip at $40cm/s$ (VSE-355G2) 85
3.25 Spurious resonances at high frequency (VSE-355G2) 86
3.26 Teleseisms: co-located VSE, STS-2 - velocity (VSE-355G2) 87
3.27 Bandpass from $100s$ to $200s$ of teleseism data (VSE-355G2) 87
3.28 FFT of teleseism data (VSE-355G2) 88

4.1 All strong motion stations in Japan 93
4.2 Strong motion stations in Hokkaido 94
4.3 GPS variation: 1 sample/day over 7 days 97
4.4 GPS variation: 1 sample/$30s$ over $12.5hr$ around M8.3 mainshock 97
4.5 GPS vs. seismometers on Hokkaido Island, M8.3: Horizontal 100
4.6 GPS vs. seismometers on Hokkaido Island: Vertical 101
4.7 GPS vs. seismometers and Accelerometers near epicenter, M8.3: Horizontal 103
4.8 GPS vs. seismometers and Accelerometers near epicenter, M8.3: Vertical . 104
4.9 GPS vs. seismometers on Hokkaido Island: Horizontal: do deconvolution . 106
4.10 GPS vs. seismometers on Hokkaido Island: Vertical: do deconvolution . . . 107

4.11 East Hokkaido map: topography and regions for investigation 110
4.12 Kushiro town stations 111
4.13 F-Net station KSR (VSE-355G2) — velocity clips 112
4.14 Kushiro town acceleration timeseries 114
4.15 Kushiro town velocity timeseries 115
4.16 Kushiro town displacement timeseries 116
4.17 Kushiro town velocity timeseries — bandpassed 117
4.18 Kushiro town displacement timeseries — bandpassed 118
4.19 Samani, Erimo region stations 119
4.20 F-Net station KMU (VSE-355G2) — velocity clips 120
4.21 Samani town acceleration timeseries 121
4.22 Samani town velocity timeseries 122
4.23 Samani town displacement timeseries 123
4.24 Samani town velocity timeseries — bandpassed 125
4.25 Samani town displacement timeseries — bandpassed 126
4.26 High-rate GPS vs. accelerometer Displacement — Mitsuishi 128
4.27 High-rate GPS vs. accelerometer Displacement — Mitsuishi — rotated . . 129
4.28 Erimo town displacement timeseries 130
4.29 Erimo town velocity timeseries — bandpassed 131
4.30 High-rate GPS vs. accelerometer displacement — Erimo1 133
4.31 High-rate GPS vs. accelerometer displacement — Erimo1 — rotated 134
4.32 Urahoro region stations 134
4.33 Urahoro acceleration timeseries 136
4.34 Urahoro velocity timeseries 137
4.35 Urahoro displacement timeseries 138
4.36 Urahoro velocity timeseries — bandpassed 139
4.37 Urahoro displacement timeseries — bandpassed 140
4.38 HKD086 liquefaction timeseries 141
4.39 HKD086 spectrogram — liquefaction 142
4.40 HKD091 spectrogram 143

4.41 Obahiro region stations 144
4.42 Obihiro displacement timeseries 146
4.43 Obihiro velocity timeseries — bandpassed 147
4.44 High-rate GPS vs. accelerometer displacement at Obihiro 148
4.45 High-rate GPS vs. accelerometer displacement — Obihiro — time synchronised 149
4.46 TKCH06 spectrogram — basin waves 150
4.47 F-Net station HID timeseries 151
4.48 Other F-Net Hokkaido stations — velocity 153
4.49 Other F-Net Hokkaido stations — displacement 154
4.50 F-Net sensors velocity comparison — M8.3 Tokachi-Oki 157
4.51 F-Net station NAA during M8.3, at 924*km* — E-W component clips 158
4.52 F-Net station NAA during M8.3 — velocity and displacement 158
4.53 F-Net station SBT during M8.3 — velocity and displacement 159
4.54 F-Net station TYM during M8.3 — velocity and displacement 159
4.55 F-Net sensors velocity comparison — M7.1 Tokachi-Oki aftershock 162
4.56 F-Net sensors velocity comparison — M6.8 off Honshu 163
4.57 F-Net station TKA during M8.3 — velocity and displacement 164
4.58 F-Net station TKD during M8.3 — velocity and displacement 164
4.59 F-Net station YMZ during M8.3 — velocity and displacement 165
4.60 F-Net velocity comparison — all data : instruments 168
4.61 F-Net velocity comparison — all data: instrument ratios 170
4.62 F-Net velocity comparison — all data: components 171
4.63 F-Net strong motion velocity vs. distance for 3 events 172

5.1 Cart Test — September 2003 (VSE-355G3) 180
5.2 Cart Test — November 2003 — tilting (VSE-355G3) 181
5.3 Cart Test — November 2003 — large velocities (VSE-355G3) 182
5.4 Tilt response — January 2004 (VSE-355G3) 184
5.5 Theoretical and observed response — VSE-355G2/3 — wide band 186

5.6 Theoretical and observed response — VSE-355G2/3 — 100s corner 187
5.7 Theoretical and observed response — VSE-355G2/3 — 3 components . . . 188
5.8 Sensitivity scaling (VSE-355G3) 190
5.9 Noise: VSE-355G3 vs. STS-2 191
5.10 San Simeon timeseries at CRP 193
5.11 Noise resolution for VSE-355G3 vs. CMG-1T 194
5.12 VSE-355G3 channel sensitivity at CRP, February 2004 196

6.1 Millikan Library from North-East 202
6.2 Millikan Library — N-S section 203
6.3 Millikan Library — plan view 203
6.4 Millikan Library natural frequency history 206
6.5 Millikan Library natural frequency vs. amplitude 207
6.6 Whittier Narrows Millikan Library records 208
6.7 Broad Center from South-West 213
6.8 Broad Center from North-West 213
6.9 Broad Center — plan view 214
6.10 Broad Center — stacked FFT data 216
6.11 MIK lifetime spectrogram 220
6.12 MIK lifetime spectrogram — no scaling 221
6.13 CBC lifetime spectrogram 222
6.14 CBC lifetime spectrogram — no scaling 223
6.15 Deviation from mean of Millikan Library natural frequencies 224
6.16 CBC lowest frequency resonance spectrograms 226
6.17 CBC lowest frequency resonance spectrograms — no scaling 227
6.18 Winter 2002-2003 at MIK 228
6.19 Effect of rainfall at MIK 229
6.20 Heavy rainfall — E-W 1^{st} and 2^{nd} modes, February 2003 — scaled 230
6.21 As Figure 6.20 — no scaling 230

6.22 Hot temperatures, high winds, rainfall — E-W 1^{st} and 2^{nd} modes, October 2003 — scaled 231
6.23 As Figure 6.22 — no scaling 231
6.24 Effect of strong winds at MIK 233
6.25 Effect of high temperature at MIK 234
6.26 Big Bear earthquake — USGS Array at Millikan Library 236
6.27 Continuous MIK Data from Big Bear - 30*s* slice spectrograms 238
6.28 Continuous MIK Data from Big Bear - 5*min* slice spectrograms 238
6.29 Continuous E-W CBC Data from Big Bear - 5*min* slice spectrograms 240
6.30 Continuous N-S CBC Data from Big Bear - 5*min* slice Spectrograms 241
6.31 Forward modelling of GSA to MIK - M2.0 event 243
6.32 Forward modelling of GSA to MIK - M5.4 Big Bear event 244

7.1 Fault model geometry 251
7.2 Simplified fault geometry 256
7.3 Arrival time azimuthal dependency 257
7.4 Convolution of 2 boxcars 258
7.5 source time function: the effect of azimuth and directivity 259
7.6 Yorba Linda and aftershocks: focal mechanisms 261
7.7 Yorba Linda: timeseries — map 263
7.8 Yorba Linda: timeseries — azimuth 264
7.9 Yorba Linda: timeseries — ordered 265
7.10 Yorba Linda: Transfer Functions from M2.85 — Transverse 266
7.11 Yorba Linda: timeseries from M2.85 — Radial 266
7.12 Yorba Linda: Transfer Functions from M2.85 — Radial 267
7.13 Yorba Linda: timeseries from M2.85 — Vertical 267
7.14 Yorba Linda: Transfer Functions from M2.85 — Vertical 268
7.15 Yorba Linda: Transfer Functions from M2.85 — all components 268
7.16 Yorba Linda: S-wave timeseries — azimuth 269
7.17 Yorba Linda: Transfer Functions from M2.85— S-wave Transverse 270

7.18 Yorba Linda: Transfer Functions from M2.85 — S-wave Radial 270
7.19 Yorba Linda: Transfer Functions from M2.85 — S-wave Vertical 271
7.20 Yorba Linda: displacement timeseries comparison with M2.66 — Transverse component 272
7.21 Yorba Linda: Transfer Functions from M2.66 — all components 272
7.22 Yorba Linda: displacement timeseries comparison with M2.93 — Transverse component 273
7.23 Yorba Linda: Transfer Functions from M2.93 — all components 273
7.24 Yorba Linda: displacement timeseries comparison with M2.47 — Transverse Component 274
7.25 Yorba Linda: Transfer Functions from M2.47 — all components 275
7.26 Yorba Linda: individual station timeseries comparison 276
7.27 Yorba Linda: individual station source time functions comparison 277
7.28 Yorba Linda: individual station source time functions comparison — scaled 278
7.29 Big Bear and aftershocks: Focal Mechanisms 279
7.30 Big Bear: Transfer Functions from M3.27 — all components 280
7.31 Big Bear: Transfer Functions from M2.92 — all components 281
7.32 Big Bear: Transfer Functions from M2.31 — all components 281
7.33 Big Bear: Transfer Functions from M2.66 — all components 282
7.34 Big Bear: Transfer Functions from M4.61 — all components 282
7.35 Big Bear: individual station source time functions comparison — scaled . . 283
7.36 Big Bear: individual station timeseries comparison 284
7.37 Anza: displacement timeseries comparison with M2.90 — E-W component 286
7.38 Anza: Transfer Functions from M2.90 — all components 287

A.1 Milling machine test data results (VSE-355G2) 298
A.2 Tilt test - using levelling screws - March 2002 (VSE-355G2) 300
A.3 VSE-355G3 Cart Test errors — March 2003 304
A.4 Elevator test (VSE-355G3) 305
A.5 Cart test — clip at 240cm/s, September 2003 (VSE-355G3) 306

A.6 Cart test — duration of a test sequence, September 2003 (VSE-355G3) . . . 307
A.7 Calibration coil response test, September 2003 (VSE-355G3) 309
A.8 Tilt test — using levelling screws, October 2003 (VSE-355G3) 310
A.9 Tilt test — using levelling screws, November 2003 (VSE-355G3) 312
A.10 Battery test, November 2003 (VSE-355G3) 313
A.11 Cart test — duration of test sequence, November 2003, with re-levelling (VSE-355G3) 314
A.12 Tilt test, using levelling screws, January 2004 (VSE-355G3) 316

B.1 Millikan Library natural frequency history 318

C.1 Millikan Library frequency sweep - E-W shake 324
C.2 Millikan Library frequency sweep - N-S shake 324
C.3 EW 1 modeshapes 326
C.4 NS 1 modeshapes 327
C.5 Torsional modeshapes 327
C.6 Higher-order modeshapes 328

List of Tables

2.1 Typical CISN instrumentation 25
2.2 Typical CISN digitisers 27
2.3 Instrument comparisons 32
2.4 Summary of waveform data 35

3.1 Typical station gains 49
3.2 Typical broadband sensor constants 53

4.1 Summary of F-Net station performance within 1000km of Tokachi-Oki . . 160
4.2 F-Net station performance summary 166
4.3 F-Net station performance summary (continued) 167

6.1 History of Millikan Library test results - fundamental flexural modes 204
6.2 Millikan Library and Broad Center natural frequencies 212

B.1 History of Millikan Library test results, 1967-1987 319
B.2 History of Millikan Library test results, 1987-2003 320
B.3 References for historical data 321

C.1 Millikan Library forced vibration results 325